Serb. Astron. J. № 182 (2011), 17 - 24
DOI: 10.2298/SAJ1182017K

UDC 524.7–82–48–335.3
Original scientific paper

SPECTRAL PROPERTIES OF AGN WITH VERY WEAK [O III] LINES

J. Kovačević

Astronomical Observatory Belgrade, Volgina 7, 11060 Belgrade 38, Serbia
E–mail: *jkovacevic@aob.bg.ac.rs*

(Received: May 11, 2011; Accepted: May 20, 2011)

SUMMARY: The spectral properties of a sample of 58 Active Galactic Nuclei (AGN) spectra, in which emission [O III] $\lambda\lambda$4959, 5007 Å lines are weak or totally absent, are analyzed. In order to investigate the physical reason for the [O III] emission suppression, the spectral properties of the weak [O III] spectra sample are compared with the same properties of a sample of 269 spectra with the strong [O III] lines. The spectra are obtained from Sloan Digital Sky Survey (SDSS) Database. It is found that the objects with the weak or absent [O III] $\lambda\lambda$4959, 5007 Å lines generally have the high continuum luminosities (log(λL_{5100}) $>$ 45), that they are very rare at smaller redshifts ($z < 0.3$) and that they usually have strong starburst influence. From the sample with weak or absent [O III] lines, two boundary subgroups may be distinguished: the subgroup with a strong Hβ narrow component and subgroup with a very weak or negligible Hβ narrow component. The physical causes for the [O III] lines suppressing are probably different in these two subgroups: the [O III] lines are absent in objects with strong narrow Hβ probably because of strong starburst (SB) activity, which produces high density of the gas, while in the objects with the negligible narrow Hβ, the reason for [O III] and narrow Hβ suppression may be a low covering factor.

Key words. galaxies: active – galaxies: emission lines

1. INTRODUCTION

Investigation of the AGN spectral properties and correlations between them may help in solving some of the many open questions about AGN geometry, as well as about physical and kinematical properties of the AGN emission regions.

There are many unexplained correlations and trends which are found between some spectral properties in AGNs. Some of them are anticorrelations between the equivalent widths (EWs) of the emission lines and continuum luminosity: as continuum luminosity increases, the EWs of the majority of the emission lines decrease (so-called Baldwin effect, see Baldwin 1977). The physical cause of the "Eigenvector 1" set of correlations from the paper Boroson and Green (1992), is still an open question, as well. Some of the correlations which are part of the Eigenvector 1 are: as EW [O III] lines decrease, the FWHM Hβ decreases as well, but the equivalent widths of the optical Fe II lines increase.

In addition, the optical iron lines are very interesting for investigation since they correlate with many other spectral properties, and the physics behind some of these correlations are still not explained, as well as the geometrical location of the Fe II emission region. There are indications that Fe II lines originate in the Intermediate Line Region (ILR), because of correlations found between the kinematical properties of Fe II lines and the ILR component of the Balmer lines (see Marziani and Sulentic 1993, Popović et al. 2004, 2009, Kovačević et al. 2010).

On the other hand, some of the most frequently analyzed lines in AGN spectra are the [O III] $\lambda\lambda$4959, 5007 Å lines, which are usually very prominent, but in some cases, especially in narrow line Sy1 galaxies, they may be very weak. They originate from the Narrow Line Region (NLR), and they are a forbidden doublet. Since they arise in collisional excitation, their strength depends on the temperature and gas electron density n_e. It is observed that [O III] lines have very large range of equivalent widths in AGNs, which may differ by a factor of >300 (Baskin and Laor 2005). Baskin and Laor (2005) proposed that the strength of [O III] lines depends on the covering factor, electron density of the Narrow Line Region and ionization parameter U. The covering factor is set by the spatial distribution of the gas in the NLR, by the angular distribution of the illuminating ionizing radiation, and it may have the most important role in modulating the EW [O III] line strength (Baskin and Laor 2005). Also, EW of [O III] lines may be an indicator of the AGN orientation, with respect to the torus opening angle, i.e. the [O III] equivalent width may be influenced by the absorption (see Caccianiga and Severgnini 2011).

Furthermore, it is possible that the strength of the [O III] $\lambda\lambda$4959, 5007 Å lines varies with evolution of AGNs. Lipari and Terlevich (2006) have explained some properties of AGN by an "evolutive unification model". In this model, the accretion arises from the interaction between nuclear starbursts and supermassive black hole. Thus, young AGN have compact and faint Narrow Line Region (NLR), strong Fe II lines and lines from the Broad Line Region (BLR) do not have large widths. In contrast, old AGNs have extended and bright NLR, weak Fe II lines and the broad lines have greater velocity widths.

In this paper we analyze a sample in which emission [O III] $\lambda\lambda$4959, 5007 Å lines are weak or totally absent. The question is which physical cause is behind the weak emission or non-existence of the [O III] lines in these spectra? We approach this problem by analyzing the spectral properties in the sample with weak [O III] lines (EW $[\mathrm{O\ III}]_{5007} < 5$ Å). Then, the results are compared with the same properties obtained from the sample with significant [O III] line strength (EW $[\mathrm{O\ III}]_{5007} > 5$ Å).

2. THE SAMPLE AND ANALYSIS

The sample with weak [O III] lines (EW $[\mathrm{O\ III}]_{5007} < 5$ Å) contains 58 AGN spectra. From that number, 33 spectra are taken from the sample used in the paper Kovačević et al. (2010; hereafter K2010). The sample of the AGNs used in K2010 is taken from SDSS (Sloan Digital Sky Survey), Data Release 7 (for details of selection procedure, see K2010). From the 302 spectra in the sample, only 33 of them satisfy the criteria that EW $[\mathrm{O\ III}]_{5007} < 5$ Å, while the rest of 269 spectra have EW $[\mathrm{O\ III}]_{5007} > 5$ Å.

The remaining 25 spectra (from the 58 spectra sample) are chosen directly from the SDSS, Data Release 7 (Abazajian et al. 2009) using selection criteria which enable obtaining the spectra with weak [O III] lines. The spectra are selected using an SQL search query, with following requirements:

(i) signal to noise ratio (S/N > 15),
(ii) good pixel quality,
(iii) high redshift confidence (zConf > 0.95) and with z < 0.7, in order to cover the optical Fe II lines,
(iv) presence of the [O III] and the broad Hβ emission lines (EW $[\mathrm{O\ III}]_{5007}$ >0 and EW Hβ >0),
(v) $[\mathrm{O\ III}]_{5007}/\mathrm{H}\beta < 0.056$ (in order to obtain the sample with weak or negligible [O III] emission).

In this way, 48 spectra are obtained. All spectra which have strong noise in Fe II lines, as well as those which have EW $[\mathrm{O\ III}]_{5007}$ line slightly stronger than 5 Å, are rejected. Thus, we obtained 25 spectra with EW $[\mathrm{O\ III}]_{5007} < 5$ Å. The requirements (ii), (iii) and (iv) are the same as the search requirements used in K2010, while the requirement (i) for the signal to noise ratio, was higher for the K2010 sample (S/N > 20). The sample from K2010 also had additional requirement of negligible EWs of typical stellar absorption lines in order to select the spectra with small host galaxy starlight contribution.

For the 25 spectra obtained from the SDSS, the same procedure as in K2010 is used for the extinction correction, continuum removing and fitting of the lines.

The spectra are corrected for Galactic extinction using an empirical extinction function computed for each spectrum on the basis of Galactic extinction coefficients given by Schlegel (1998). The continuum emission is subtracted by DIPSO software, following the continuum windows given in paper Kuraszkiewicz et al. (2002).

After that, all emission lines in $\lambda\lambda$4400-5500 Å range (Fe II, [O III], Hβ and He II λ4686 Å) are fitted with Gaussian functions (Popović et al. 2004). Each Gaussian is described with 3 parameters: the width, intensity and shift from the transition wavelength. The iron lines are fitted by a constructed template from the paper K2010. Hβ lines, and in some cases narrow [O III] lines are fitted with the sum of Gaussians, which represent the emission from different emission regions. The different kinematical properties of those regions are reflected in different widths and shifts of Gaussians which fit one line. The Hβ line is decomposed in three components: NLR, ILR and VBLR (emission from Narrow, Intermediate and Very Broad Line Region), and fitted with three Gaussians. Each of the [O III] lines ([O III]λ 4959 Å and [O III]λ 5007 Å) are fitted with one Gaussian which has the same width and shift as Hβ NLR, and one additional Gaussian, which fits the asymmetry. Both components of the doublet [O III]λ 4959 Å and [O III]λ 5007 Å have the same shape, but their intensity ratio is approximately 1:2.99 (Dimitrijević et al. 2007). The example of the fit may be seen in papers K2010, Kovačević and Popović (2010) and Popović et al. (2009).

The shifts and the widths of Gaussians are obtained directly as fit parameters, equivalent widths and Full Width at Half Maximum (FWHM) are measured from the spectra, and continuum luminosity is calculated using the formula given in Peebles (1993), with adopted cosmological parameters: $\Omega_M = 0.27$, $\Omega_\Lambda = 0.73$ and $\Omega_k = 0$, and Hubble constant $H_o = 71$ $\mathrm{kms^{-1}Mpc^{-1}}$. Procedure of emission line decomposition, fitting of lines and obtaining the line parameters is the same as described in K2010 in details.

The FWHM is measured for the total [O III]λ 5007 Å line (sum of two Gaussians), and for the broad component of the Hβ (sum of the ILR and VBLR components).

3. RESULTS

In this section we present the main results of the comparisons between spectral and kinematical properties of two samples: with weak [O III] lines (EW $[\mathrm{O\ III}]_{5007} < 5$ Å) which contains 58 spectra, and with stronger [O III] lines (EW $[\mathrm{O\ III}]_{5007} > 5$ Å) which contains 269 spectra from K2010.

3.1. Comparison between the spectral properties of two samples

Some characteristics of the two samples (with weak and stronger [O III] lines) are compared in Fig. 1. It is interesting that the selection of spectra with weak [O III] lines gives the spectra with high continuum luminosity at 5100 Å. Namely, only 7% of spectra from weak [O III] sample have $\log(\lambda L_{5100}) < 45$, while in the sample with EW $[\mathrm{O\ III}]_{5007} > 5$ Å, 30% of spectra have luminosity lower than $\log(\lambda L_{5100}) < 45$ (Fig. 1, middle).

These results are in accordance with the Baldwin effect of [O III] lines, i.e. it is expected that the spectra with low EWs of [O III] lines have high continuum luminosities and vice versa.

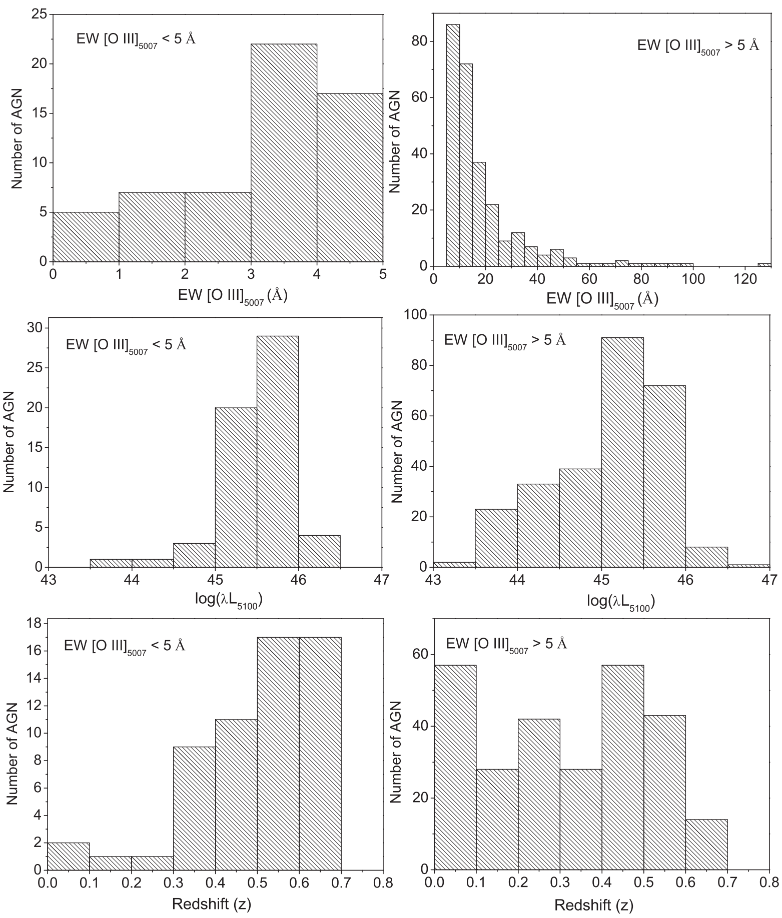

Fig. 1. *The distribution of AGN with respect to their [O III]$_{5100}$ equivalent width (top), continuum luminosity (middle) and redshift (bottom) in the samples with weak [O III] (left) and stronger [O III] lines (right).*

Also, it is noticed that the selection of spectra with weak [O III] lines corresponds to AGN with z >0.3, while only 4 objects (from 58) have z <0.3 (see Fig. 1, bottom).

Furthermore, the sample with weak or absent [O III] lines could be separated in the three subgroups according to the strength of the Hβ narrow component relative to [O III] lines: the subgroup with significant strength of Hβ NLR component (hereafter designated as S1), containing 17 objects, the subgroup in which Hβ NLR is absent or at the level of noise (hereafter designated as S2), containing 20 objects, and the rest of the objects from the weak [O III] sample (21 objects) which have the Hβ NLR approximately equally strong as [O III] lines.

The subsample with the Hβ NLR component significantly stronger than [O III] (S1) and subsample with negligible narrow Hβ component (S2) are specially interesting since it is noticed that spectra from these subsamples have some different characteristics (see Fig. 2). The spectra from the subsample with strong Hβ NLR (S1) generally have the broad component of Hβ (ILR + VBLR) which is narrower than in the spectra from the subsample with negligible Hβ NLR (S2). Also, the Hβ broad component does not have asymmetry in the subsample with strong Hβ narrow line (S1), while in the subsample in which the Hβ narrow line is negligible (S2), the broad Hβ usually have a significant red asymmetry. The examples of the typical spectra from the subsamples S1 and S2, are shown in the Fig. 2. These two types of objects have probably different physical properties, and it is possible that the absence of [O III] lines in their spectra is caused by different reasons.

In order to investigate the differences between samples with strong and week [O III] lines, as well as between subsamples S1 and S2 from weak [O III] sample, the possible influence of the starburst activity is analyzed. Namely, it is possible that an AGN spectrum in an earlier activity phase is composed of the starburst and of the central engine (pure AGN) spectrum (Croom et al. 2002, Lipari and Terlevich 2006, Wang and Wei 2006, 2008, Mao et al. 2009, Popović et al. 2009).

Since there are no complete measurements of line parameters which are needed for the construction of the starburst/AGN diagnostic BPT diagram (Baldwin, Phillips and Terlevich 1981), the criterium $R=\log([\mathrm{O\ III}]_{5007}/\mathrm{H}\beta\ \mathrm{NLR})=0.5$ is adopted as an indicator of the predominant starburst emission contribution to the narrow emission lines (see Popović and Kovačević 2011, Kovačević and Popović 2010). Namely, we assume that objects with R>0.5 have the AGN activity dominant, while objects with R<0.5 have dominant the starburst activity.

The distributions of the AGNs versus $R=\log([\mathrm{O\ III}]_{5007}/\mathrm{H}\beta\ \mathrm{NLR})$ ratio are shown in Fig. 3 for samples with strong and week [O III] lines as well as for subsamples S1 and S2. Majority of objects (∼3/4) from the stronger EW [O III] sample have R >0.5, which indicates domination of AGN activity in these objects, while approximately 1/4 of the spectra from that sample have R <0.5, which indicates the SB domination (Fig. 3, a). On the contrary, in the weak [O III] sample, only approximately 1/4 of the spectra are AGN dominated while majority of objects (∼3/4) are dominated by the starburst activity (Fig. 3, b). Considering the weak [O III] subsamples, the objects from the subsample with strong Hβ NLR (S1) are all SB dominated (R <0.5) which is shown in Fig. 3 (c), while objects with negligible Hβ NLR (S2) have similar distribution as the sample with stronger [O III] lines (Fig. 3, d).

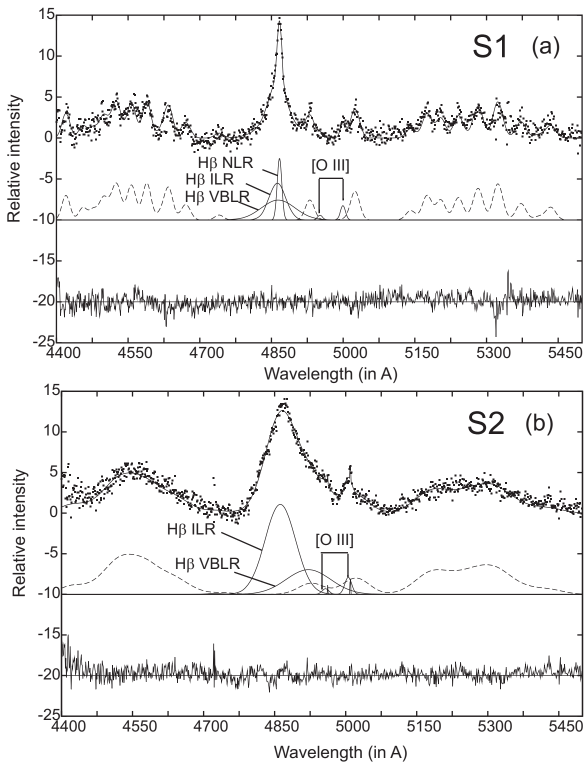

Fig. 2. *The examples of the spectra with weak [O III] and: (a) strong and (b) negligible Hβ NLR. The Fe II template is denoted by dashed line.*

3.2. Comparison between the kinematical spectral properties

The kinematical properties (shifts and Doppler widths) of the Hβ components (NLR, ILR and VBLR), Fe II lines, as well as FWHM of Hβ broad and $[\mathrm{O\ III}]_{5007}$, are compared between the sample with the weak [O III] lines and the sample with significant strength of [O III] lines.

Also, the kinematical properties are analyzed for two subgroups with specific characteristics which are distinguished from the sample with weak [O III] lines, and which represent the two boundary cases (S1 and S2 subgroups).

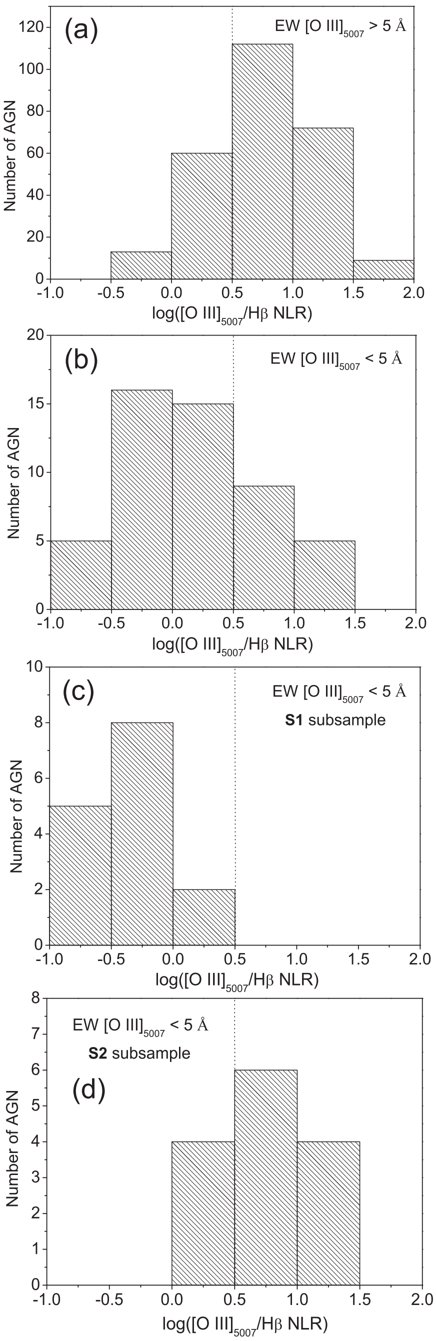

Fig. 3. *The distribution of the AGN versus R=log([O III]$_{5007}$/Hβ NLR) ratio for the sample with significant [O III] strength (a), the total weak [O III] sample (b), and subsamples S1 and S2 (c and d, respectively). The ratio R=0.5 is denoted by dashed line.*

The average values of widths and shifts are shown in Tables 1 and 2. Since Hβ NLR and [O III] are inside the noise level in some objects, it was not possible to measure their properties in the whole sample. The properties of Hβ NLR are measured in 53 objects (17 objects from S1 and 15 objects from S2) and the FWHM [O III] in 54 objects (15 objects from S1 and 18 objects from S2).

It could be seen that the average FWHM of the broad Hβ (ILR + VBLR), as well as the average Doppler widths of the Hβ broad components separately (ILR and VBLR) in the S1 subsample are very close to the corresponding average widths in the EW [O III]$_{5007}$ > 5 Å sample (FWHM Hβ: ∼3200 km/s, Hβ ILR: ∼1600 km/s and Hβ VBLR: ∼4400 km/s). On the other hand, the subsample with very weak narrow Hβ (S2), has significantly larger corresponding widths of the broad Hβ (by approximately ∼1000 km/s) when compared to S1 and EW [O III]$_{5007}$ > 5 Å samples. The average width of the iron lines is larger in the S2, as well. Furthermore, the S2 subsample has more redshifted broad Hβ components (ILR and VBLR) when compared to S1 and EW [O III]$_{5007}$ > 5 Å sample. This is especially emphasized in the case of Hβ VBLR where average shift value in S2 is 2410±1390 km/s, which is approximately ∼1300 km/s larger than in the EW [O III]$_{5007}$ > 5 Å sample, and for ∼1800 km/s larger than in the S1 subsample.

On the contrary, the average widths of the narrow lines (Hβ NLR Doppler width and FWHM [O III]$_{5007}$) are broader in the S1 subsample (∼500 km/s for Hβ NLR and ∼1200 km/s for [O III]$_{5007}$), than in the subsample with very weak Hβ NLR (S2) and the sample with EW [O III]$_{5007}$ > 5 Å, in which the average widths of the narrow lines are approximately the same (∼250 km/s for Hβ NLR and ∼750 km/s for [O III]$_{5007}$). The narrow Hβ lines are generally more redshifted in the S1 subsample, than in the S2 and EW [O III]$_{5007}$ > 5 Å samples.

The Fe II lines are slightly more redshifted in both the S1 and S2 subsamples (∼280 km/s), when compared to the EW [O III]$_{5007}$ > 5 Å sample (∼180 km/s).

4. DISCUSSION AND CONCLUSIONS

In this paper, the AGN spectra with weak [O III] lines (EW [O III]5007 < 5 Å) are investigated, and the spectral properties from weak-[O III] sample are compared with the same properties from the sample with significant strength of the [O III] lines (EW [O III]$_{5007}$ > 5 Å).

It is interesting that almost all spectra considered as having the weak [O III] lines have high luminosity (log(λL_{5100}) > 45) and redshift higher than 0.3. Continuum luminosity is strongly correlated with cosmological redshift in our sample because of the selection effect since for the higher redshifts, the objects with higher luminosity are observed. Since it is difficult to separate luminosity from the evolutionary effect in our sample, a further investigation is necessary to check whether the weak [O III] lines are connected with the AGN evolution.

Table 1. The kinematical properties of the Hβ in analyzed samples. The widths and shifts are given in km/s.

	FWHM	width			shift		
	Hβ	Hβ NLR	Hβ ILR	Hβ VBLR	Hβ NLR	Hβ ILR	Hβ VBLR
EW [O III]$_{5007}$ < 5 Å (all)	3640±1340	380±220	1815±730	4640±1440	210±190	150±190	1450±1420
S1 subsample	3270±880	500±200	1660±500	4480±1340	280±120	130±200	600±800
S2 subsample	4650±1390	220±150	2370±730	5410±1520	170±230	220±210	2410±1390
EW [O III]$_{5007}$ > 5 Å	3150±1440	290±140	1550±710	4320±1440	160±130	110±240	1100±1430

Table 2. The kinematical properties of the [O III] and Fe II in analyzed samples. The widths and shifts are given in km/s.

	FWHM [O III]	width Fe II	shift Fe II
EW [O III]$_{5007}$ < 5 Å (all)	940±460	1560±590	250±240
S1 subsample	1210±500	1120±300	280±100
S2 subsample	790±380	2060±600	270±380
EW [O III]$_{5007}$ > 5 Å	740±470	1430±440	180±300

It is found that in the sample with weak [O III] lines, two boundary groups can been distinguished: the spectra with weak [O III] lines but with strong Hβ narrow lines, and the spectra with weak [O III] lines and almost absent Hβ NLR (S1 and S2, respectively).

Since these two groups have many different spectral characteristics (they differ in widths and shifts of the broad and narrow lines), it is possible that objects belonging to these two groups have significantly different kinematical and physical properties, i.e. that the reasons for weakening of the [O III] lines in these objects have different origin.

It is possible that the main reason for the weak [O III] lines in the S1 subsample, which has strong narrow Hβ NLR, is a high density (n_e) of the NLR gas. Namely, if the gas density is close to the critical density for forbidden [O III] lines, it will result in very weak [O III] lines, because of the collisional suppression, but it will have no influence on Hβ NLR, since it is a pure recombination line (Baskin and Laor 2005). On the other hand, the high density could be a consequence of the starburst activity, i.e. the violent star-forming events in the nucleus (Netzer et al. 2004). The distribution of the R=log([O III]$_{5007}$/Hβ NLR) ratio for the S1 subsample supports this possibility, since all objects have R <0.5, which is an indicator of predominant starburst contribution. Also, the narrow lines (especially [O III]) which are broader in the S1 than in the S2 subsample and the sample with strong [O III] lines, indicate higher stellar velocities, since [O III] line width is correlated with the stellar velocity distribution in the bulge (Nelson 2000, Shields et al. 2003).

The case of the objects which belong to the S2 subgroup is especially interesting. These objects, which have a weak [O III] lines and almost absent Hβ NLR lines, have very broad and significantly redshifted broad Hβ components, as well as the large width of the Fe II lines. This is not in accordance with Boroson and Green's (Boroson and Green 1992) Eigenvector 1 set of correlations, in which it is found that as [O III] lines decrease, the width of the broad Hβ decrease as well. It is possible that in the case of the S2 subsample, the main reason for the weak [O III] lines is the low covering factor of the NLR gas, i.e. some kind of the disappearing NLR which may be one phase in the AGN evolution. Namely, the Hβ NLR lines are very sensitive to the covering factor (Baskin and Laor 2005), which means that a low covering factor may result in low [O III] and Hβ NLR lines. In this sample, the majority of the objects have the AGN activity dominant, while only a small fraction have dominant the SB activity, as well as in the sample with strong [O III] lines.

From this investigation, the following conclusions may be outlined:

(1.) The objects with the weak or absent [O III] $\lambda\lambda$4959, 5007 Å lines generally have high continuum luminosities (log λL_{5100} > 45) and these objects are very rare at smaller redshifts (z <0.3),

(2.) The objects with the weak or absent [O III] lines generally have strong starburst influence, and majority of objects in the sample are SB dominant (∼3/4). On the contrary, in the sample with significant strength of the [O III] lines (EW [O III] > 5 Å), the majority of objects are AGN dominant (∼3/4), while only ∼1/4 of objects have strong SB influence,

(3.) From the objects which have weak or absent [O III] lines, the two boundary cases may be distinguished: the objects with strong Hβ NLR (S1), and the objects with negligible Hβ NLR line (S2). The objects with strong Hβ NLR have no asymmetry in the Hβ broad component, they have relatively broad lines from the Narrow Line Region and they are all starburst dominated. The objects with negligible Hβ NLR line, have very broad and redshifted Hβ lines (ILR and VBLR component) and they are generally AGN dominated,

(4.) The objects with weak or absent [O III] lines from the S1 and S2 subgroups probably have different reasons for suppressing the [O III] emission: the [O III] lines are absent in objects with strong Hβ NLR probably because of the strong SB activity which produces a high density of gas, while in the objects with negligible Hβ NLR, the reason for [O III] and Hβ NLR suppression may be in a low covering factor.

Acknowledgements – This work is a part of my PhD thesis supervised by Dr. Luka Č. Popović, who pointed out the problem of the weak [OIII] lines in AGN. This work also makes part of the project "Astrophysical Spectroscopy of Extragalactic Objects" (176001) supported by Ministry of Education and Science of Serbia.

REFERENCES

Abazajian, K. N. et al.: 2009, *Astrophys. J. Suppl. Series*, **182**, 543A.
Baldwin, J. A.: 1977, *Astrophys. J.*, **214**, 679.
Baldwin, J. A., Phillips, M. M., Terlevich, R., 1981, *Publ. Astron. Soc. Pacific*, **93**, 5.
Baskin, A. and Laor, A.: 2005,*Mon. Not. R. Astron. Soc.* , **358**, 1043.
Boroson, T. A. and Green, R. F.: 1992, *Astrophys. J. Suppl. Series*, **80**, 109.
Caccianiga, A., Severgnini, P.: 2011, *Mon. Not. R. Astron. Soc.*, accepted.
Croom, S. M., Rhook, K., Corbett, E. A. et al.: 2002, *Mon. Not. R. Astron. Soc.*, **337**, 275.
Dimitrijević, M. S., Popović, L. Č., Kovačević, J., Dačić, M., Ilić, D.: 2007,*Mon. Not. R. Astron. Soc.*, **374**, 1181.
Kovačević, J. and Popović, L. Č.: 2010, *Publ. Astron. Obs. Belgrade*, **89**, 367.
Kovačević, J., Popović, L. Č., Dimitrijević, M. S.: 2010, *Astrophys. J. Suppl. Series*, **189**, 15.
Kuraszkiewicz, J. K., Green, P. J., Forster, K., Aldcroft, T. L., Evans, I. N. and Koratkar, A.: 2002, *Astrophys. J. Suppl. Series*, **143**, 257.
Lipari, S. L. and Terlevich, R. J.: 2006, *Mon. Not. R. Astron. Soc.*, **368**, 1001.
Mao, Y-F., Wang, J., Wei, J.-Y.: 2009, *Astron. Astrophys.*, **9**, 529.
Marziani, P. and Sulentic, J. W.: 1993, *Astrophys. J.*, **558**, 553.
Nelson, C. H.: 2000, *Astrophys. J.*, **544**, L91.
Netzer, H., Shemmer, O., Maiolino, R., Oliva, E., Croom, S., Corbett, E., di Fabrizio, L.: 2004, *Astrophys. J.*, **614**, 558.
Peebles, P. J. E.: 1993, Principles of Physical Cosmology, Princeton University Press, Princeton.
Popović, L. Č. and Kovačević, J.: 2011, *Astrophys. J.*, accepted (arXiv: 266110).
Popović, L. Č., Mediavilla, E., Bon, E. and Ilić, D.: 2004, *Astron. Astrophys.*, **423**, 909.
Popović, L. Č., Smirnova, A., Kovačević, J., Moiseev, A. and Afanasiev, V.: 2009, *Astron. J.*, **137**, 3548.
Schlegel, M.: 1998, *Astrophys. J.*, **500**, 525.
Shields, Gregory A., Gebhardt, Karl, Salviander, Sarah, Wills, Beverley J., Xie, Bingrong, Brotherton, Michael S., Yuan, Juntao, Dietrich, Matthias: 2003, *Astrophys. J.*, **583**, 124.
Wang, J., Wei, J.: 2006, *Astrophys. J.*, **648**, 158.
Wang, J., Wei, J.: 2008, *Astrophys. J.*, **679**, 86.

СПЕКТРАЛНЕ ОСОБИНЕ АГЈ СА ВЕОМА СЛАБИМ [O III] ЛИНИЈАМА

J. Kovačević

Astronomical Observatory Belgrade, Volgina 7, 11060 Belgrade 38, Serbia

E–mail: *jkovacevic@aob.bg.ac.rs*

UDK 524.7–82–48–335.3

Оригинални научни рад

Анализиране су спектралне особине узорка од 58 активних галактичких језгара (АГЈ) у којем су [O III]$\lambda\lambda$4959, 5007 Å линије слабе или потпуно одсутне. У циљу истраживања физичког разлога слабе емисије [O III], спектралне особине узорка са слабим [O III] линијама су упоређене са истим особинама АГЈ узорка од 269 спектара са значајном јачином [O III] линија. Спектри су преузети из Sloan Digital Sky Survey (SDSS) базе. Примећено је да објекти са слабим или одсутним [O III] $\lambda\lambda$4959, 5007 Å линијама углавном имају високе луминозности континуума ($\log(\lambda L_{5100}) > 45$), ретко се налазе на малим црвеним помацима ($z < 0.3$) и углавном имају јак утицај региона у којима се интензивно формирају звезде. У узорку са слабим [O III] линијама, могу се издвојити две граничне подгрупе: подгрупа са јаком уском Hβ компонентом и подгрупа са врло слабом или занемарљивом уском Hβ компонентом. Физички разлог слабе емисије [O III] линија у ова два подузорка је вероватно различит: [O III] линије су слабе у објектима са јаком уском Hβ вероватно због појачане активности у регионима у којима се интензивно формирају звезде, што повећава густину гаса, док у објектима са занемарљивом уском Hβ линијом, разлог слабе емисије [O III] и уске Hβ, могао би бити слаб фактор покривања, тј. мало гаса у усколинијском региону.